Thioredoxin Reductase−Thioredoxin Fusion Enzyme from *Mycobacterium leprae*: Comparison with the Separately Expressed Thioredoxin Reductase†

Pan-Fen Wang,‡,§ Jovita Marcinkeviciene,§,|| Charles H. Williams, Jr.,‡,⊥ and John S. Blanchard*,||

Department of Biochemistry, Albert Einstein College of Medicine, Bronx, New York 10461, Department of Biological Chemistry, University of Michigan, Ann Arbor, Michigan 48109, and Department of Veterans Affairs Medical Center, Ann Arbor, Michigan 48105

Received April 2, 1998; Revised Manuscript Received September 14, 1998

ABSTRACT: Thioredoxin reductase (TrxR) catalyzes the reduction of thioredoxin (Trx) by NADPH. A unique gene organization of TrxR and Trx has been found in *Mycobacterium leprae*, where TrxR and Trx are encoded by a single gene and, therefore, are expressed as a fusion protein (MlTrxR−Trx). This fusion enzyme is able to catalyze the reduction of thioredoxin or 5,5′-dithiobis(2-nitrobenzoic acid) or 1,4-naphthoquinone by NADPH, though the activity is much lower than that of *Escherichia coli* TrxR. It has been proposed that a large conformational change is required in catalysis of *E. coli* TrxR. Because the reductase portion of the enzyme from *M. leprae* shows significant primary structure similarity with *E. coli* TrxR, it is possible that MlTrxR−Trx may require a similar conformational change and that the change in conformation may be affected by the tethered Trx. The reductase has been expressed without Trx attached (MlTrxR). As reported here, comparison of the steady-state and pre-steady-state kinetics of MlTrxR−Trx with those of MlTrxR suggests that the low reductase activity of the fusion enzyme is an inherent property of the reductase, and that any steric limitation caused by the attached thioredoxin in the fusion protein makes only a minor contribution to the low activity. Titration of MlTrxR−Trx and MlTrxR with 3-aminopyridine adenine dinucleotide phosphate ($AADP^+$), an NADP(H) analogue, results in only slight quenching of FAD fluorescence, suggesting an enzyme conformation in which the binding site of $AADP^+$ is not close to the FAD, as in one of the conformations of *E. coli* TrxR.

The thioredoxin system comprising the flavoprotein thioredoxin reductase (TrxR),[1] thioredoxin (Trx), and NADPH operates to transfer reducing equivalents in the reductive half-reaction from NADPH to the noncovalently bound FAD and finally to the redox-active cysteine residues in TrxR. The subsequent transfer of reducing equivalents to the low molecular weight redox protein thioredoxin occurs in the oxidative half-reaction via dithiol exchange of reduced thioredoxin reductase and oxidized thioredoxin to generate oxidized thioredoxin reductase (disulfide form) and reduced thioredoxin (dithiol form) (*1*−*4*). Reduced thioredoxin provides reducing equivalents to a wide variety of metabolic pathways and regulatory proteins, such as the synthesis of deoxyribonucleotide (*5*) and sulfate metabolism (*6*). Both the high and low molecular weight forms of the flavoprotein thioredoxin reductase are members of the pyridine nucleotide disulfide oxidoreductase family (*7*). Other members of this family include lipoamide dehydrogenase and glutathione reductase (*1*).

The structure of the related enzyme glutathione reductase reveals a clear path of electron flow from NADPH to the substrate glutathione via flavin and active site disulfide, with the flavin ring separating the pyridine nucleotide binding site on the *re* side from the redox-active disulfide on the *si* side (*8*−*10*). *E. coli* TrxR is the best studied low molecular weight form of thioredoxin reductase (*1*). In contrast to the clear path of electron flow in glutathione reductase, the X-ray structure of *E. coli* TrxR shows that the redox-active disulfide composed of Cys135 and Cys138 is adjacent to the *re* face of the isoalloxazine ring of the FAD, interposed between FAD and the nicotinamide ring of the bound NADPH (*11*, *12*). This conformation is favorable for electron transfer between the flavin and the disulfide and is called the FO conformation, standing for flavin oxidation by enzyme disulfide (Scheme 1). However, the substrate thioredoxin appears to be unable to approach the buried enzyme dithiol in the FO conformation, and the location of the bound

† This work was supported by NIH Grants GM21444 (C.H.W.) and GM33449 (J.S.B.), and by the Health Services and Research Administration of the Department of Veterans Affairs (C.H.W.).

* To whom correspondence should be addressed. Phone: (718) 430-3096. FAX: (718) 430-8565.

‡ University of Michigan.

§ Both authors contributed equally to this work. Present address for Dr. Jovita Marcinkeviciene: DuPont Pharmaceuticals, E400/3221, P.O. Box 80400, Route 141 & Henry Clay Rd., Wilmington, DE 19880.

|| Albert Einstein College of Medicine.

⊥ Department of Veterans Affairs Medical Center.

[1] Abbreviations: TrxR, thioredoxin reductase; Trx, thioredoxin; MlTrxR−Trx, fusion enzyme of thioredoxin reductase and thioredoxin from *Mycobacterium leprae*; MlTrxR, truncated enzyme which is the separately expressed thioredoxin reductase from *Mycobacterium leprae*; MlTrxR+Trx, reconstituted system where soluble thioredoxin has been added to truncated *Mycobacterium leprae* thioredoxin reductase; $AADP^+$, 3-aminopyridine adenine dinucleotide phosphate; DTNB, 5,5′-dithiobis(2-nitrobenzoic acid); DTT, 1,4-dithiothreitol; TEA, triethanolamine; NQ, 1,4-naphthoquinone; FO, observed conformation of *E. coli* thioredoxin reductase in which flavin oxidation by the redox-active disulfide is favored; FR, putative conformation of thioredoxin reductase in which flavin reduction by NADPH is favored.

10.1021/bi980754e CCC: $15.00
Published on Web 10/30/1998

Scheme 1: Representations of *E. coli* and *M. leprae* TrxR in FO and Postulated FR Conformers[a]

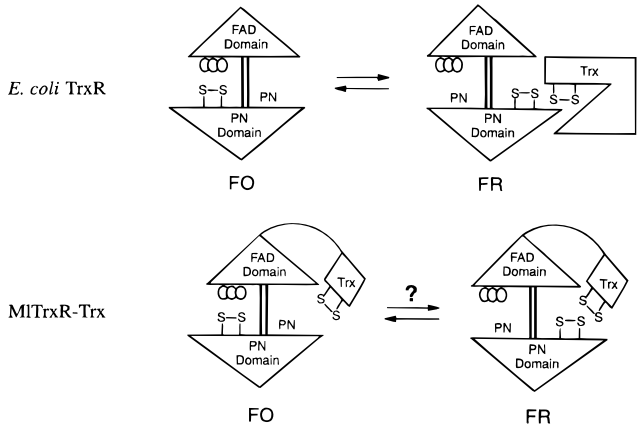

[a] FAD and pyridine nucleotide domains are indicated and connected by lines depicting the double-stranded β-sheet. The three circles represent FAD, and PN indicates bound pyridine nucleotide. Although the difference between the FO and FR conformers is shown as a 180° rotation in this illustration, the rotation is actually postulated to be 66°.

NADPH does not allow hydride transfer between the nicotinamide ring and the flavin. These structural characteristics led to the proposal that a conformational change is required during catalysis by *E. coli* thioredoxin reductase (*12*). If the NADPH domain is fixed, and the FAD domain is rotated 66°, the nicotinamide ring of NADPH would be in close contact with the FAD, and the active site dithiol would be moved to the surface of the protein where it is accessible to the substrate thioredoxin. This conformation is referred to as the FR conformation which stands for flavin reduction by NADPH (Scheme 1). A body of indirect evidence supports this putative conformational change of *E. coli* TrxR (*13*−*18*).

The genes encoding thioredoxin reductase (*trxB*) and thioredoxin (*trxA*) have been characterized from a number of pro- and eukaryotes, and in essentially all organisms, the two genes are located at distant sites on the genome. An unprecedented gene organization has recently been described in the bacterial pathogen *Mycobacterium leprae* (*19*, *20*). In this slow-growing, intracellular pathogen, TrxR and Trx are encoded by a single gene in which the 2 protein-coding regions are linked via a 22 amino acid connecting sequence (Scheme 1). *M. leprae* is the causative agent of leprosy, and is phagocytized by, and can proliferate in, human macrophages. The pathogenicity of mycobacteria is critically dependent on their ability to survive inside the oxidatively challenging macrophage phagolysosome. Since the normal, physiological functions of the thioredoxin system include reactivation of protein thiols (*21*) and detoxifying reactive oxygen species (*22*), it is tempting to speculate that the TrxR−Trx systems of intracellular pathogens, including mycobacterial species, may play a significant role in their resistance to oxygen-dependent killing mechanisms employed by phagocytes.

In this paper we report the cloning and expression of the wild-type *M. leprae* TrxR−Trx, the individual thioredoxin reductase domain, MlTrxR, and also *M. tuberculosis* thioredoxin. Steady-state kinetic and isotopic analyses of the reactions catalyzed by MlTrxR−Trx and MlTrxR have been compared in this study. This includes the determination of the pH dependence of the reductions of naphthoquinone, DTNB, and thioredoxin catalyzed by MlTrxR−Trx, MlTrxR alone, and MlTrxR+Trx (Scheme 2). The combination of these data with primary deuterium and solvent kinetic isotope effect studies has yielded information on the rate-limiting nature of the half-reactions that contribute to catalysis. The spectral characteristics, redox properties, and pre-steady-state kinetics for the fusion protein (MlTrxR−Trx) and the separately expressed MlTrxR have been compared. The results indicate that both forms of the enzyme are in a conformation in which the binding site of NADPH is not close to FAD, i.e., a conformation similar to the FO conformation of the *E. coli* thioredoxin reductase (Scheme 1). The question whether the low reductase activity of the *M. leprae* fusion enzyme is an inherent property of the reductase, or results from steric limitation imposed by the attached thioredoxin, has been addressed.

MATERIALS AND METHODS

Reagents. NADPH, 3-aminopyridine adenine dinucleotide phosphate ($AADP^+$), 5,5′-dithiobis(2-nitrobenzoic acid) (DTNB), and sodium dithionite were purchased from Sigma Chemical Co. *E. coli* thioredoxin was prepared as previously described (*13*). All other reagents and buffer salts were of the highest quality available. Protocatechuic acid and protocatechuic acid dioxygenase were kind gifts from Dr. D. P. Ballou, University of Michigan.

Overexpression and Purification of Wild-Type MlTrxR−*Trx, the Truncated MlTrxR Domain, and Trx Proteins in E. coli.* The fused *trxAB* gene of *M. leprae* (*19*) was amplified from genomic *M. leprae* DNA by PCR using primers containing *Nde*I and *Bam*HI restriction sites at the 5′ and 3′ ends, respectively. The PCR product was digested with these two enzymes and ligated into a pET-3a overexpression vector (Novagen) previously digested with *Nde*I and *Bam*HI. The resulting plasmid was used to transform BL21(DE3) *E. coli* (Novagen). The separate *M. leprae* thioredoxin reductase enzyme-expressing gene was engineered by introducing a stop codon immediately preceding the first codon of the 22 amino acid linker (determined by alignment of the *M. leprae* and *M. tuberculosis trxAB* and *trxB* genes, respectively) connecting the TrxR and Trx domains of the wild-type enzyme (*19*). Similar procedures were employed in the PCR amplification, ligation, and transformation of the engineered MlTrxR gene. A construct for the expression of the *Mycobacterium tuberculosis* thioredoxin, which is a separate gene in this species encoding a nearly identical protein to *M. leprae* thioredoxin, was prepared using this same strategy.

Expression of all three proteins (MlTrxR−Trx, MlTrxR, and Trx) was performed in *E. coli* by the addition of 0.5 mM isopropyl β-thiogalactopyranoside to cultures in mid-log growth phase. After overnight culturing at 22 °C, the cells were harvested, resuspended in 20 mM triethanolamine (TEA) hydrochloride, pH 7.8, and disrupted by sonication, and the supernatant obtained after centrifugation was treated with streptomycin sulfate (1% w/v final) to remove nucleic acids. The supernatant obtained after one more centrifugation was dialyzed and applied to a Fast Flow Q Sepharose (Pharmacia) anion-exchange column preequilibrated in 20 mM TEA-HCl, pH 7.8, and eluted with a linear 0.2−0.6 M NaCl gradient. Fractions exhibiting NADPH-dependent

Scheme 2

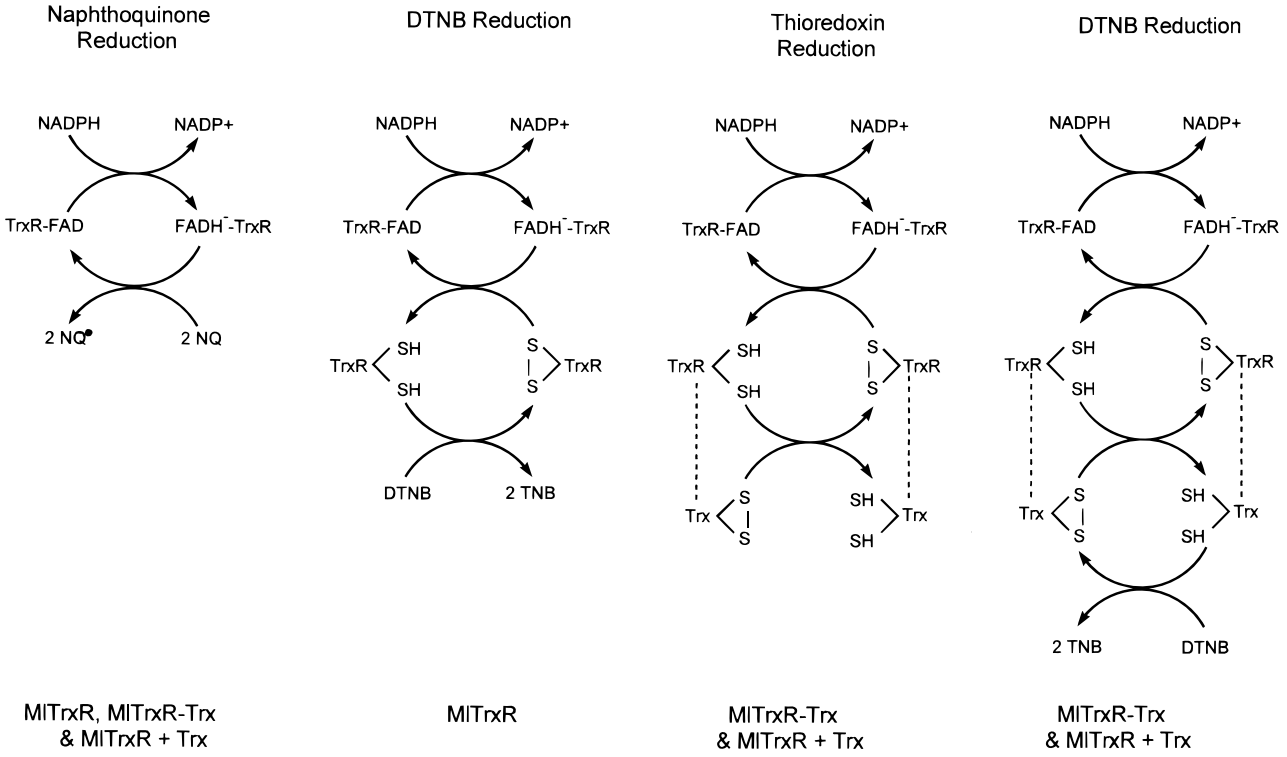

reduction of DTNB were pooled, concentrated, made 1 M in ammonium sulfate by the addition of solid $(NH_4)_2SO_4$, and applied to a Phenyl Superose (Pharmacia) column. Adsorbed protein was eluted with a nonlinear 1−0 M reverse ammonium sulfate gradient. Active fractions eluting between 0.2 and 0.1 M $(NH_4)_2SO_4$ were pooled, concentrated to 5 mL, and applied to a 1.6 × 60 cm Superdex 200 (Pharmacia) gel filtration column to remove minor contaminating species. The purification protocol for MlTrxR and Trx used the same chromatographic steps with minor variations in elution conditions, and Trx was assayed in fractions by determining the Trx-dependent oxidation of NADPH by purified MlTrxR. The purified enzyme used in pre-steady-state experiments was stored at −20 °C in 20 mM TEA buffer, 2 mM DTT, and 50% glycerol. Removal of glycerol and changing of buffers were effected with an Amicon Centricon concentrator (Beverly, MA).

The activity of the fused or separate thioredoxin reductases during purification was determined by measuring the rate of reduction of 0.5 mM DTNB at 412 nm ($\epsilon_{412} = 13.6$ mM^{-1} cm^{-1}) in the presence of 0.1 mM NADPH, and additionally in the presence of added Trx for MlTrxR. Naphthoquinone reduction was measured by following the oxidation of NADPH at 340 nm ($\epsilon_{340} = 6.2$ mM^{-1} cm^{-1}). The concentration of reductase active sites, both MlTrxR−Trx and MlTrxR, was calculated based on the absorbance of FAD at 455 nm, using an extinction coefficient of 11.3 mM^{-1} cm^{-1}. The expressed enzymes were subjected to 12−20 cycles of amino-terminal sequencing using an Applied Biosystem Sequencer using Edman degradation chemistry.

Thiol Alkylation Studies. The alkylation of reduced MlTrxR−Trx was performed by anaerobically incubating a mixture of 5 μM reductase, 0.2 mM NADPH, and 2 mM iodoacetamide for 1 h. Reduction of either DTNB or naphthoquinone was measured as described above.

pH Profiles. The following buffers at 0.1 M concentration were used: succinate (5.0−6.0), phosphate (6.0−8.0), carbonate (8.0−9.5). Wild-type enzyme, MlTrxR−Trx, was inhibited by a number of organic buffers, including MES, PIPES, HEPES, TAPS, EPPS, and POPSO, and the highest activity was observed in phosphate buffer. The kinetic parameters V and V/K were determined at each pH, and their log values were plotted against pH. The data were fitted to the appropriate equation, using the programs of Cleland (*23*).

$$\log Y = \log [C/(1 + H^+/K_a + K_b/H^+)] \quad (1)$$

$$\log Y = \log [C/(1 + H^+/K_a)] \quad (2)$$

$$\log Y = \log [Y_L + Y_H(K/H^+)/(1 + K/H^+)] \quad (3)$$

$$\log Y = \log [C/(1 + K_b/H^+)] \quad (4)$$

Data for pH profiles that decreased at high and low pH values with slopes of −1 and 1, respectively, were fit to eq 1. Data for pH profiles that decreased with a slope of 1 at low pH values were fit to eq 2. Data for pH profiles that decreased from a pH-independent value at high pH values to a lower, pH-independent value at low pH values were fit to eq 3, where Y_L and Y_H are the pH-independent values of the kinetic parameter at low and high pH, respectively. Data for pH profiles that decreased with a slope of −1 at high pH values were fit to eq 4.

Isotope Effects. [4S-4-^{1}H]- and [4S-4-^{2}H]-NADPH were prepared and purified as described previously (*24*). Oxidation of NADPH was monitored spectrophotometrically at 340 nm using an extinction coefficient of 6.2 mM^{-1} cm^{-1}. Experiments which yielded primary kinetic isotope effects on V only, or on both V and V/K, were fit to eqs 5 and 6,

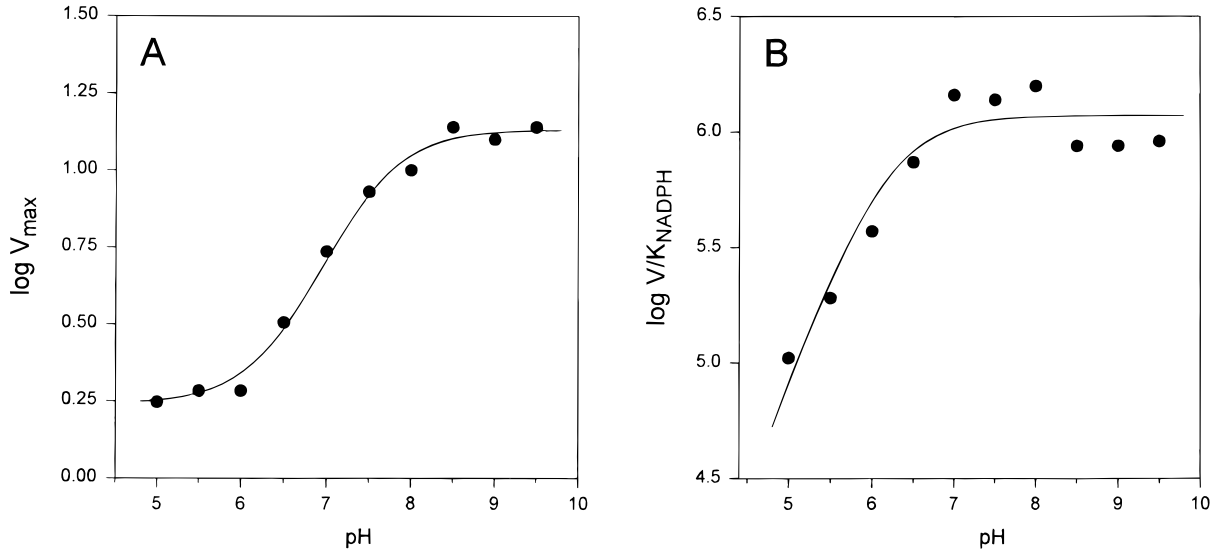

FIGURE 1: *Mycobacterium leprae* wild-type thioredoxin reductase−thioredoxin-catalyzed reduction of 1,4-NQ: pH dependence of the V_{max} (A) where the smooth curve is the fit of the data to eq 3 and yielded a pK value of 7.4 ± 0.2, and V/K_{NADPH} (B) where the smooth curve is the fit of the data to eq 4 and yielded a pK value of 6.2 ± 0.2.

respectively, where A is the substrate concentration, F_i is the fraction of deuterium label, and E_V and $E_{V/K}$ are the isotope effect minus 1 on V and V/K, respectively.

$$v = VA/[K + A(1.0 + F_iE_V)] \quad (5)$$

$$v = VA/[K(1.0 + F_iE_{V/K}) + (1.0 + F_iE_V)] \quad (6)$$

Solvent Kinetic Isotope Effects. Reaction mixtures containing NADPH, Trx, or NQ and the desired isotopic solvent composition were prepared in 1 mL cuvettes. Proton inventory experiments were performed by measuring the initial velocity of NADPH oxidation at various mole fractions of D_2O from 0.0 to 0.9. The velocities were plotted against the mole fraction of D_2O, and the resulting plots were used to estimate the number of protons transferred, and the solvent kinetic isotope effects on either V, V/K, or both.

Extinction Coefficient. The extinction coefficients of MlTrxR−Trx and MlTrxR were determined as described previously (*25*). Enzyme samples in 50 mM TEA buffer, pH 7.6, were denatured with 31.8 mM SDS and incubated at 40 °C for 40 min. The amount of released FAD was quantitated spectrophotometrically using an extinction coefficient of 11.3 mM^{-1} cm^{-1} at 450 nm.

Sodium Dithionite Titrations. Titrations of MlTrxR−Trx and MlTrxR with sodium dithionite were performed using the method described previously (*26*). Anaerobic sodium dithionite solution was prepared in 50 mM pyrophosphate buffer, pH 9.0, and quantitated by anaerobic titration of lumiflavin-3-acetic acid. Enzyme samples (16−32 μM) in 0.1 M Na/K PO_4 or 50 mM TEA buffer, pH 7.6, were titrated with dithionite at 25 °C anaerobically in the presence of 10% methyl viologen (relative to FAD) which acts as a mediator of the reducing equivalents.

AADP$^+$ Fluorescence Titration. Enzymes (7−8 μM) in 0.1 M Na/K PO_4, pH 7.6 and 25 °C, contained in a fluorescence cuvette were titrated aerobically with AADP$^+$. After each addition of AADP$^+$, corrected fluorescence spectra were recorded on a Perkin-Elmer MPF-44B fluorimeter.

Rapid Reaction Spectrophotometry. The rapid reaction spectrophotometry and the pre-steady-state kinetic data analysis were performed as described previously (*13*). The anaerobiosis of the stopped-flow instrument was achieved by equilibration with an anaerobic solution of 80 μM protocatechuic acid and 0.04 unit/mL protocatechuic acid dioxygenase in 0.1 M Na/K PO_4, pH 7.6, for at least 4 h. TrxR−Trx (16 μM) in 0.1 M Na/K PO_4, pH 7.6, was made anaerobic by alternate exposure to vacuum and reequilibration with ultrapure nitrogen, and used to fill one stopped-flow syringe. Protocatechuic acid (80 μM) and 0.04 unit/mL protocatechuic acid dioxygenase were included in the enzyme solution to remove trace oxygen. The solution of NADPH (1, 3, or 9 equiv relative to enzyme-bound FAD) in the same buffer was bubbled with nitrogen for 10 min before being used to fill the other syringe. The two solutions were mixed rapidly at 4 °C. Kinetic traces at 456 and 540 nm (photomultiplier detector) and spectra (diode array detector) were collected. The enzyme solution was protected from light during anaerobiosis and reduction. In experiments involving anaerobiosis, EDTA was omitted from the buffers because it potentiates photoreduction of the *E. coli* enzyme. When the kinetic traces at 540 nm were analyzed using Program A (Dr. D. P. Ballou, University of Michigan), the fitted curves were extrapolated back for the dead time (2.3 ms) of the stopped-flow instrument, and the rate constant for the first phase was varied until the extrapolated starting absorbance of the fitted curve matched the observed starting absorbance of the oxidized enzyme.

RESULTS

Alkylation Studies. Anaerobic incubation of 5 μM MlTrxR−Trx with iodoacetamide led to the loss of 90% of the DTNB reducing activity (which could not be restored upon the addition of thioredoxin), while the quinone reducing activity was not affected (data not shown).

pH Dependence of the Kinetic Parameters for the NQ Reduction Reaction. The pH profiles shown in Figure 1 were obtained using variable concentrations of NADPH at a saturating concentration of NQ. The maximum velocity is

Table 1: Comparison of V_{max} Values of the Reactions Catalyzed by *M. leprae* Thioredoxin Reductase−Thioredoxin and Thioredoxin Reductase

	V_{max} (s^{-1})		
enzyme	NADPH-dependent reduction of added Trx	NADPH-ependent reduction of NQ	NADPH-dependent reduction of DTNB
MlTrxR−Trx	1.8 ± 0.1	19 ± 0.9	1.4 ± 0.1
MlTrxR	2.1 ± 0.1	15 ± 0.2	0.1 ± 0.01

highest at alkaline pH values (Figure 1A) and decreases to a lower, pH-independent value at lower pH values, as a group exhibiting a pK value of 7.4 ± 0.2 is protonated. The pH dependence of V/K_{NADPH} (Figure 1B) is highest at high pH values, and decreases as a group exhibiting a pK value of 6.2 ± 0.2 is protonated.

pH Dependence of the Kinetic Parameters for the Reduction of DTNB by MlTrxR−Trx, MlTrxR+Trx, and MlTrxR. Both MlTrxR and MlTrxR−Trx catalyzed the NADPH-dependent reduction of DTNB, though at different rates (Table 1). The pH dependence of the rate of DTNB reduction catalyzed by MlTrxR−Trx, MlTrxR+Trx, and MlTrxR was examined using DTNB as the variable substrate at high, saturating concentrations of NADPH (100 μM) at pH values between 4.5 and 9.5. The pH dependencies of the maximum velocities for the reactions catalyzed by MlTrxR−Trx and MlTrxR+Trx were similar, exhibiting the highest values when a group exhibiting a pK value of 8.0 ± 0.4 was protonated and a group exhibiting a pK value of 5.9 ± 0.4 was deprotonated (Figure 2A). The maximum velocity of DTNB reduction catalyzed by MlTrxR increases modestly at high pH values, with the rate depending on protonation of a group exhibiting a pK value of 7.1 ± 0.2.

The pH dependences of V/K_{DTNB} catalyzed by MlTrxR−Trx or MlTrxR were almost identical to those observed for the pH dependence of the maximum velocity, while the pH dependence of V/K_{DTNB} catalyzed by MlTrxR+Trx exhibits pH-independent V/K_{DTNB} values in the region of pH 5−8, and decreases as a group exhibiting a pK value of 8.5 ± 0.3 is deprotonated (Figure 2B).

Solvent Kinetic Isotope Effects. Solvent kinetic isotope effect studies were determined using both MlTrxR−Trx and MlTrxR in three different reactions: reduction of DTNB, NQ, or Trx (Scheme 2). No solvent kinetic isotope effects were observed in the NQ reduction reactions (Table 2), while the reductions of both DTNB and Trx were sensitive to solvent isotopic composition. When DTNB was varied at a fixed, saturating concentration of NADPH in H_2O and D_2O, no isotope effects were observed on V/K_{DTNB}, but large changes in V were observed in D_2O (Figure 3A). The calculated values of V, determined at various mole fractions of D_2O, were plotted against the mole fraction of D_2O and yielded a linear proton inventory (Figure 3B). Similar studies performed at various Trx concentrations, and at a fixed, saturating concentration of NADPH, yielded solvent kinetic isotope effects on both V and V/K_{Trx} (Table 2), and the magnitudes of these two effects were similar for both MlTrxR−Trx and MlTrxR.

Primary Deuterium Kinetic Isotope Effects. Large primary kinetic isotope effects on both V and V/K_{NADPH} were observed for the reduction of NQ catalyzed by MlTrxR−Trx and MlTrxR, using NADPH and [4S-^{2}H]NADPH as variable substrates (Table 2). Smaller primary kinetic isotope effects on both V and V/K_{NADPH} were observed when the rate of reduction of Trx catalyzed by MlTrxR−Trx and MlTrxR was evaluated (Table 2).

Sodium Dithionite Titrations. According to the primary structure, MlTrxR−Trx contains two disulfides; one is the active site disulfide in the TrxR, and the other one is the active site disulfide in the substrate Trx. The proposed electron flow in catalysis is from NADPH to FAD, from $FADH_2$ to the active disulfide in the TrxR, followed by an intramolecular dithiol/disulfide interchange reaction in which the reducing equivalents are passed to the active site disulfide of the Trx. Therefore, a reductive titration of MlTrxR−Trx should require 3 equiv of dithionite per FAD for full reduction. On the other hand, the truncated enzyme MlTrxR, lacking the substrate Trx and the peptide linker, would need 2 equiv of dithionite per FAD for full reduction.

The dithionite titration of the truncated enzyme MlTrxR (Figure 4) demonstrated that, as expected, 2 equiv of dithionite is required for complete reduction (Figure 4, inset A). The titration appeared to be biphasic or curved, indicating that the redox potentials of the flavin and disulfide couples are similar (*27*). The production of a small amount of neutral semiquinone was evident at 575 and 625 nm (*3*). The final spectrum showed peaks near 610 and 395 nm indicative of methyl viologen radical, as expected when the enzyme is fully reduced. A small excess of dithionite was suggested at 315 nm. The enzyme was reoxidized by opening the cuvette to air after the dithionite titration. The mixture was concentrated with an Amicon Centricon 30 ultrafiltration unit, and ∼24% free FAD was found in the filtrate. Flavin dissociation is not observed in *E. coli* thioredoxin reductase or in other members of this enzyme family.

The reductive titration of MlTrxR−Trx with dithionite is qualitatively similar to that for MlTrxR presented in Figure 4, and the quantitation is shown in Figure 4, inset B. The first addition of dithionite (0.46 equiv) resulted in a lag in flavin reduction (see below). The absorbance at 456 nm decreased linearly upon the next two additions (from 0.46 to 1.37 equiv), while the subsequent additions gave proportionately smaller decreases in A_{456}. After addition of 4.6 equiv of dithionite, the spectrum displayed high absorbance at 395, 610, and 315 nm, indicating the presence of methyl viologen radical and excess dithionite (spectrum not shown). The plot of ϵ_{456} versus equivalents of dithionite (Figure 4, inset B) showed the lag in flavin reduction mentioned above that indicated 0.4 equiv of residual oxygen. The end point of the titration was 3.9 equiv. After correction for the 0.4 equiv lag and 0.1 equiv for methyl viologen, the amount of dithionite required for full reduction of MlTrxR−Trx is 3.4 equiv, which was close to the expected 3 equiv. As shown in Figure 4, inset B, it is obvious that there are two phases during the dithionite titration of the fusion enzyme. The first phase is from 0.4 to 1.6 equiv in which about 51% of flavin is reduced. The rest of the flavin was reduced in the second phase which is from 1.6 to 3.9 equiv. A small amount of neutral semiquinone was formed and reduced during the titration (575 and 625 nm). As with the truncated enzyme, about 25% of the FAD was released during the experiment.

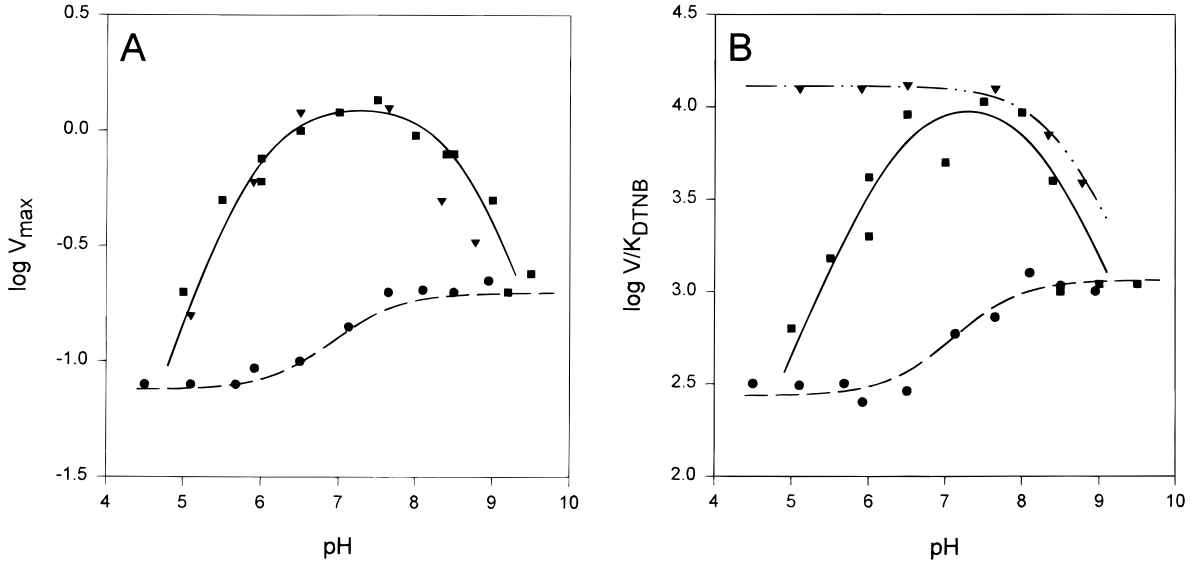

FIGURE 2: pH dependence of the V_{max} (A) and V/K_{DTNB} (B) for DTNB reduction by *Mycobacterium leprae* MlTrxR−Trx (■), MlTrxR (●), and MlTrxR + 20 μM Trx (▼). The smooth curves are fits of the data to eqs 1 (solid curves), 2 (dash−dot), and 3 (dashed). The p*K* values determined from these fits are reported in the text.

Table 2: Comparison of Isotope Effects of the Reduction of NQ and Trx Catalyzed by MlTrxR−Trx and MlTrxR

enzyme	isotope effect	NADPH-dependent reduction of added Trx	NADPH-dependent reduction of NQ
MlTrxR−Trx	solvent	$^{D2O}V = 2.7 \pm 0.3$ $^{D2O}V/K_{Trx} = 1.6 \pm 0.3$	no effect
MlTrxR	solvent	$^{D2O}V = 2.3 \pm 0.1$ $^{D2O}V/K_{Trx} = 1.8 \pm 0.2$	no effect
MlTrxR−Trx	primary deuterium	$^{D}V = 1.1 \pm 0.1$ $^{D}V/K_{NADPH} = 1.0 \pm 0.1$	$^{D}V = 3.3 \pm 0.1$ $^{D}V/K_{NADPH} = 2.1 \pm 0.2$
MlTrxR	primary deuterium	$^{D}V = 1.8 \pm 0.1$ $^{D}V/K_{NADPH} = 1.4 \pm 0.3$	$^{D}V = 3.7 \pm 0.1$ $^{D}V/K_{NADPH} = 3.1 \pm 0.6$

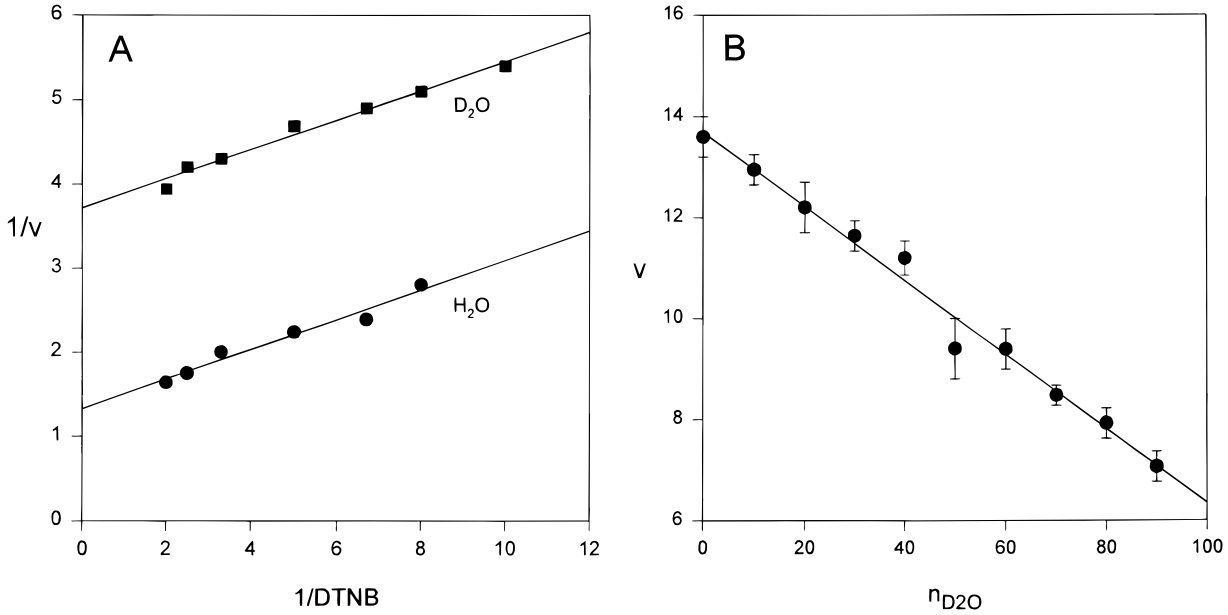

FIGURE 3: (A) Solvent kinetic isotope effect on DTNB reduction catalyzed by *M. leprae* wild-type TrxR−Trx using 0.1 mM NADPH and variable [DTNB]. (B) Dependence of the rate of DTNB reduction on the mole fraction of D_2O. [NADPH] = 0.1 mM, [DTNB] = 0.4 mM. The ^{D2O}V calculated from these data was 2.1 ± 0.1.

Since the shoulder at 480 nm, which is prominent in the enzyme and much less distinct in FAD, was maintained throughout the titration, it is suggested that FAD dissociation occurs during enzyme reoxidation.

Reduction of MlTrxR−Trx and MlTrx with NADPH. Reduction of MlTrxR and MlTrxR−Trx with NADPH has been studied using a stopped-flow spectrophotometer. Single-wavelength kinetic traces are shown in Figure 5A for the reaction of MlTrxR with 3 and 9 equiv of NADPH. The kinetic trace at 456 nm showed that a lag lasting for about 10 ms followed the dead time (2.3 ms). A_{456} decayed in three phases with the observed rate constants shown in Table

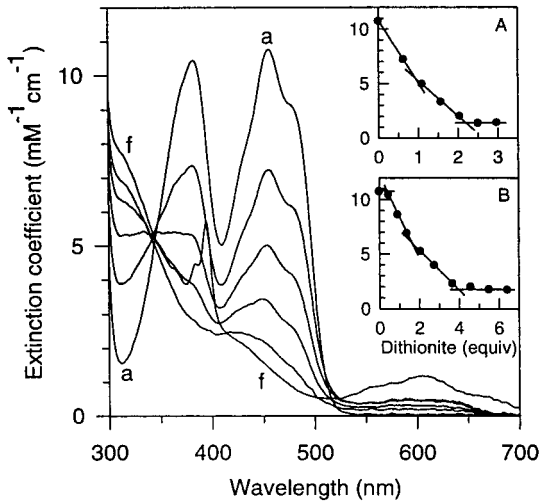

FIGURE 4: Titration of MlTrxR with sodium dithionite. A solution of 36.9 nmol MlTrxR in 1.2 mL of 50 mM TEA buffer, pH 7.6, containing 3.69 nmol of methyl viologen was titrated anaerobically with 2.88 mM sodium dithionite at 25 °C. The spectra are of the mixture after addition of 0, 0.62, 1.09, 1.56, 2.03, and 2.50 equiv of sodium dithionite (a−f). Inset A, plot of A_{456} versus equiv of sodium dithionite for MlTrxR. Inset B, plot of A_{456} versus equiv of sodium dithionite for MlTrxR−Trx.

Table 3: Observed Rates for the Reduction of MlTrxR−Trx and MlTrxR by NADPH[a]

enzyme	wavelength (nm)	k_1 (s^{-1})	k_2 (s^{-1})	k_3 (s^{-1})	k_4 (s^{-1})	k_5 (s^{-1})
MlTrxR	456	−	12.5	2.62	0.49	−
	540	419	46.6	3.51	1.19	0.21
	540[b]	834	60.3	3.15	1.02	0.26
MlTrxR−Trx	456	−	21.2	3.40	0.69	−
	540	247	40.8	3.07	−	0.12
	540[b]	410	103	2.92	−	0.18
E. coli TrxR C138S[c]	456	425	60	9		

[a] The values are the observed rates for the reactions with 3 equiv of NADPH. [b] The traces were fitted with k_1 determined as described under Materials and Methods. [c] Reference *15*.

3. The final phase was still in progress at the end of data collection (10 s).

The absorbance at 540 nm was monitored to follow the formation and decay of the NADPH−FAD charge-transfer complex observed in the previous studies with the *E. coli* enzyme (*13*, *28*−*29*). A_{540} increased in two phases during the first 40 ms after mixing and decreased biphasically for about 3 s. A further phase was observed in the reduction with 3 equiv of NADPH. This was probably due to the slow formation of the $FADH^-$−$NADP^+$ charge-transfer complex and was not observed with 9 equiv because the pyridine nucleotide binding site was occupied by NADPH. The formation of the NADPH−flavin charge-transfer complex might be expected to be dependent on the NADPH concentration. The dependence of k_1 on the NADPH concentration was observed only when the data were fitted by varying k_1 until the extrapolated starting absorbance of the fitted curve matched the observed starting absorbance of the oxidized enzyme. Even then, the nature of the dependence was not clear. This is not surprising given the complexity of the reductive half-reaction studied in detail with the *E. coli* enzyme (*13*−*15*). No concentration dependence could be shown for any of the other rate constants.

The spectra collected during the reduction of MlTrxR by 3 equiv of NADPH are presented in Figure 5B. The dead time spectrum has a long-wavelength band centered around 570 nm which looks very similar to the NADPH−FAD charge-transfer complex band observed with *E. coli* TrxR. The dead time spectrum also shows a slight enhancement of the flavin shoulder around 482 nm, but it has almost the same absorbance at 456 nm as oxidized enzyme. The spectrum at 13 ms still displays little signal change of the flavin peak (456 nm) with further enhancement of the shoulder, and further formation of the charge-transfer complex. In the next phase, the flavin peak is reduced while the long-wavelength band is enhanced slightly (spectrum at 100 ms). Both the flavin peak and long-wavelength band

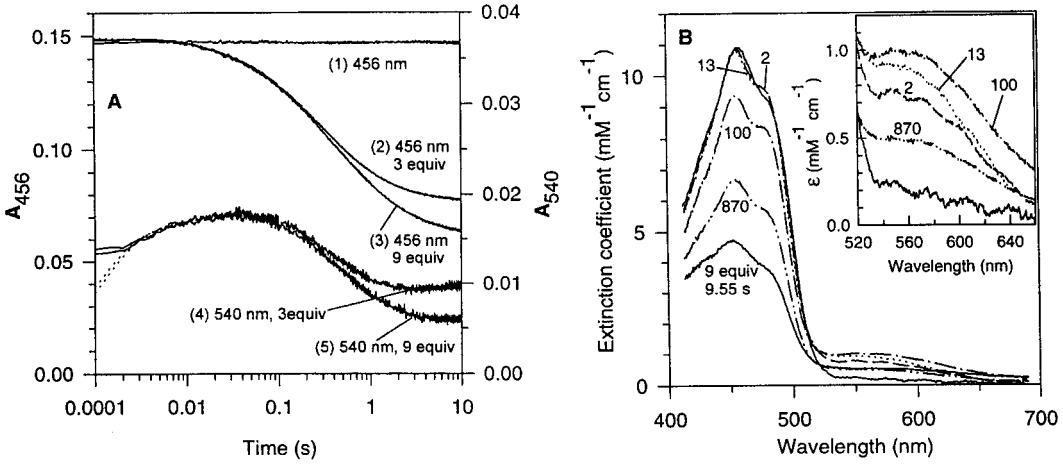

FIGURE 5: Rapid reaction of MlTrxR with NADPH. MlTrxR (13 μM after mixing) was reduced by 3 and 9 equiv of NADPH in 0.1 M Na/K PO_4 at pH 7.6 and 4 °C. (A) Single-wavelength kinetic traces. Curve 1 is the trace of oxidized enzyme mixed rapidly with buffer to illustrate the starting absorbance at 456 nm. Curve 2 (456 nm) and curve 4 (540 nm) are from the reaction with 3 equiv of NADPH. Curve 3 (456 nm) and curve 5 (540 nm) are from the reaction with 9 equiv of NADPH. The data are fitted with three exponentials (456 nm) or four exponentials (540 nm) as indicated by the dotted lines. The traces at 540 nm are fitted with the k_1 held constant as described under Materials and Methods. (B) Spectra taken during the reduction of MlTrxR by NADPH. The spectra are of oxidized enzyme mixed with buffer (solid line) and oxidized enzyme mixed with 3 equiv of NADPH after 2.3 ms (dead time, dashed line), 13 ms (dotted line), 100 ms (dash and dotted line), and 870 ms (dash and double-dotted line). The final spectrum from the reaction with 9 equiv of NADPH is also presented (solid line with lowest flavin peak). The inset shows the detail of the long-wavelength band.

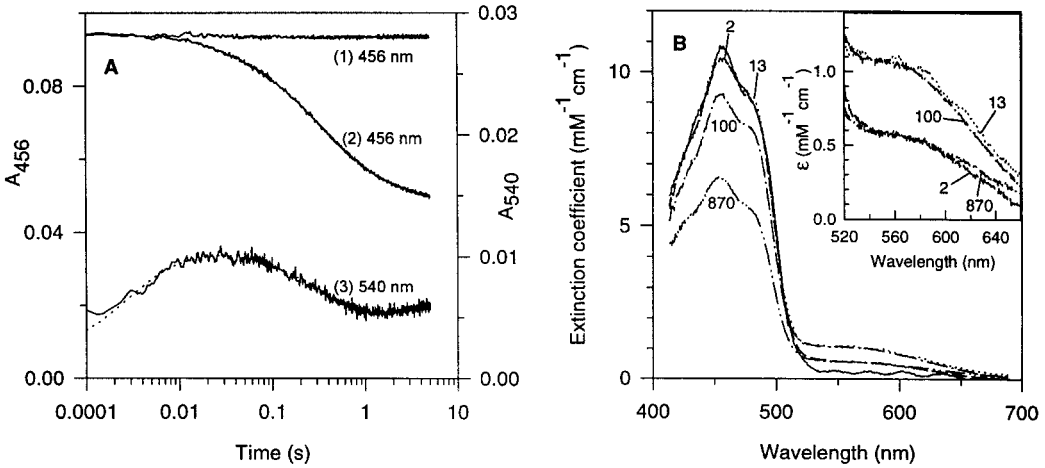

FIGURE 6: Rapid reaction of MlTrxR−Trx with NADPH. MlTrxR−Trx (8 μM after mixing) was reduced by 3 equiv of NADPH in 0.1 M Na/K PO_4 at pH 7.6 and 4 °C. (A) Single-wavelength kinetic traces. Curve 1 is the trace of oxidized enzyme mixed rapidly with buffer to illustrate the starting absorbance at 456 nm. The reduction of MlTrxR−Trx by NADPH was observed at 456 nm (curve 2) and 540 nm (curve 3). The data are fitted with three exponentials (456 nm) or four exponentials (540 nm) by indicated in the dotted lines. The trace at 540 nm is fitted with k_1 locked as described under Materials and Methods.. (B) Spectra taken during the reduction of MlTrxR−Trx by NADPH. The spectra are of oxidized enzyme mixed with buffer (solid line) and oxidized enzyme mixed with NADPH after 2.3 ms (dead time, dashed line), 13 ms (dotted line), 100 ms (dash and dotted line), and 870 ms (dash and double dotted line). The inset shows details of the long-wavelength band.

decreased from 100 to 870 ms in the main phase of flavin reduction, and continued thereafter. The final spectrum from the reduction with 9 equiv of NADPH is included for comparison.

Data for the reduction of MlTrxR−Trx by NADPH are presented in Figure 6, and Table 3. Analysis of the single-wavelength kinetic traces (Figure 6A) and the diode array spectra (Figure 6B) gives results very similar to those for the truncated enzyme.

AADP$^+$ Titrations. AADP$^+$ is a redox-inactive analogue of NADP(H) (*30*) and is thus expected to bind in the binding site of NADPH, without reducing the flavin. In the case of *E. coli* TrxR, extensive fluorescence quenching by AADP$^+$ indicates that AADP$^+$ is bound adjacent to the FAD and that the FR conformation is favored (*16*). In this study, it was found that the FAD fluorescence at 540 nm (excitation at 380 nm) of MlTrxR and MlTrxR−Trx is enhanced approximately 3-fold compared with free FAD. When titrated with AADP$^+$, the fluorescence was quenched only 19% for MlTrxR and 18% for MlTrxR−Trx (data not shown), suggesting that the FO conformation is favored. K_d values for AADP$^+$ binding were 2.9 and 5.3 μM for MlTrxR and MlTrxR−Trx, respectively.

DISCUSSION

Mycobacterium leprae is an obligate intracellular pathogen responsible for human leprosy. The recent identification of the unique genetic organization of the thioredoxin reductase and thioredoxin genes in this organism, resulting in the expression of a single fused gene product (*19*), suggested that this fused TrxR−Trx protein might provide insight into the large conformational changes which have been proposed to occur during catalysis by the related low molecular weight *E. coli* thioredoxin reductase. In contrast to high molecular weight flavoprotein disulfide reductases, such as lipoamide dehydrogenase or glutathione reductase, the three-dimensional structure of *E. coli* thioredoxin reductase revealed that both the pyridine nucleotide and redox-active disulfide must react at the same *re* face of the isoalloxazine ring of the bound FAD (*4*, *11*). This has led to the proposal that thioredoxin reductase exists in a dynamic conformational equilibrium between forms in which the pyridine nucleotide is close to the isoalloxazine ring (the FR conformation) or, alternatively, the redox-active disulfide is close to the ring (the FO conformation) (*12*). Both rapid kinetic data and extensive mutagenesis studies support this proposal (*13*−*18*), and more recent studies have suggested that in the presence of thioredoxin the *E. coli* reductase favors the FR conformation as a result of the formation of a disulfide bridge between thioredoxin and the redox-active thiols of the reductase (*17*). The report that the *M. leprae* fused thioredoxin reductase−thioredoxin, MlTrxR−Trx, exhibited a significantly slower turnover than the corresponding *E. coli* enzyme (*20*) suggested that the presence of the linked thioredoxin might be a useful probe of this conformational change. The studies performed in this work have allowed us to determine whether the low activity exhibited by the wild-type *M. leprae* is due to restricted conformation or is an intrinsic property of the enzyme found in this slow-growing organism.

pH Profiles. The simplest enzyme-catalyzed reaction studied is the thioredoxin reductase catalyzed reduction of naphthoquinone (Scheme 2). The ability of related flavoprotein reductases to catalytically reduce quinone compounds has been previously documented (*31*, *32*). Several possible mechanisms for quinone reduction exist, including mechanisms involving single electron transfer, hydride ion transfer, and dithiol reduction (*31*). The demonstration that alkylation of reduced MlTrxR−Trx with iodoacetamide abolished both the DTNB- and Trx-reducing ability of the enzyme, but had no effect on NQ reduction, suggests that enzymic dithiols are not involved in NQ reduction, as observed in other flavoprotein disulfide reductase systems (*31*−*33*). The pH dependence of V/K_{NADPH} indicates that the protonation of a substrate or free enzyme group exhibiting a pK value of 6.2 decreases this kinetic constant. The most likely explanation

for this behavior is that the ionizable group being observed is the 2′-phosphate of the substrate NADPH, whose solution p*K* value has been reported to be 6.5 (*34*). This suggests that the nucleotide binding domain of MlTrxR strongly favors the dianionic form of the 2′-phosphate for binding at the active site of the enzyme. In support of this conclusion, we could not demonstrate activity using cyclic 2′,3′-NADPH as a reductant for the reductase and NADH was a poor substrate, exhibiting a steady-state K_m value over 200 times higher than NADPH (data not shown).

The pH dependence of the maximum velocity of NQ reduction exhibits a pH-independent value at low pH values and a pH-independent maximum at higher pH values. The most likely candidate for the group whose protonation decreases the maximum velocity of quinone reduction and exhibits a p*K* value of 7.4 is the reduced, anionic flavin, $FADH^-$. The protonation state of $FADH^-$ has been suggested to be important in modulating the rate of the quinone reductase reactions catalyzed by the related flavoprotein, NADH peroxidase (*31*). The nature of potential rate-limiting steps of the NQ reduction reaction will be discussed below.

DTNB reacts with enzyme dithiols, generating the corresponding disulfides. DTNB has often been used as a substrate for disulfide reductases, and, because of the very low p*K* values of the product, *p*-nitrothiophenol, formed upon DTNB reduction, DTNB was used in this study to specifically identify enzyme groups whose behavior is observed in pH profiles. The reductase, in addition to FAD, contains a pair of cysteine residues at the active site which, when reduced, are capable of DTNB reduction. At pH 7.5, the reduction of DTNB catalyzed by MlTrxR−Trx is more than 10-fold faster than the corresponding rate catalyzed by truncated MlTrxR (Table 1 and Figure 2). This result suggests that the thioredoxin thiols are either more reactive or more readily accessible to DTNB than those of the reductase. Clearly there is redox communication between the active site dithiol and the disulfide of Trx. Additional evidence supporting this interpretation was the observation that the addition of soluble thioredoxin to the truncated thioredoxin reductase (MlTrxR) substantially increased the rate of DTNB reduction. It should be noted that *M. leprae* TrxR−Trx shows significantly slower reaction rates compared to the *E. coli* TrxR. The slowest rate constant in the reductive half-reaction catalyzed by *E. coli* TrxR is 54 s^{-1} and the overall k_{cat} is 33 s^{-1} (*29*), while we observe a value of ∼2 s^{-1} for the k_{cat} of the *M. leprae* reductase. The lower specific activity of mycobacterial lipoamide dehydrogenase compared to other bacterial lipoamide dehydrogenases has been reported (*33*).

The pH dependence of both V and V/K_{DTNB} for DTNB reduction catalyzed by MlTrxR is sigmoidal (Figure 2), with a pH-independent value at high pH for both parameters decreasing to a lower pH-independent value at low pH as the result of the protonation of an ionizable group exhibiting a p*K* value of 7.1 or 7.4, respectively. Since DTNB does not contain ionizable groups with p*K* values in this range, both pH profiles are reporting on the ionization of enzyme residues. There are two likely candidates for this group: the aspartate in the active site proposed to function as the general acid to protonate the leaving thiolate anion product (*35*), and the MlTrxR active site thiolate responsible for nucleophilic attack on the substrate disulfide. Since DTNB does not require protonation upon reduction, it would seem unlikely that the protonation state of the aspartic acid would influence the reaction. A value of 6.9 has been reported for the p*K* of the active site thiol (active site sequence: CATC) in reduced *E. coli* TrxR (*27*). The protonation of this residue would be expected to reduce its nucleophilicity, and thus reduce the rate of DTNB reduction.

The pH dependence of the kinetic parameters for DTNB reduction by MlTrxR−Trx and MlTrxR+Trx is more complicated due to the presence of either covalently bound or added thioredoxin. The interpretation of the pH dependence of these reactions requires consideration of both the thioredoxin reductase thiol ionizations and, more importantly, the necessary protonation of the dithiols of the reduced thioredoxin product. The pH dependences of the maximum velocity of DTNB reduction catalyzed by both MlTrxR−Trx and MlTrxR+Trx are bell-shaped and depend on the ionization state of two groups. The two groups exhibit p*K* values of 5.9−6.3 and 8.0, and are required to be deprotonated and protonated, respectively, for maximal activity (Figure 2A). The group exhibiting a p*K* value of 5.9 is likely to be that of thiolate anion of Trx, which, when deprotonated, initiates the nucleophilic attack on the DTNB disulfide. It has been reported that Cys32 of the *E. coli* thioredoxin (active site sequence: C_{32}GPC) exhibits a p*K* value of 6.2 (*36*).

The group exhibiting a p*K* value of 8.0 is likely to be the general acid required for protonation of the thiolate anion product of thioredoxin reduction. Site-directed mutagenesis studies provided compelling evidence that in *E. coli* thioredoxin reductase, Asp139 functions as the general acid catalyst for the dithiol−disulfide interchange reaction between TrxR and Trx (*35*). Based on this evidence, we tentatively identify the corresponding aspartate residue (Asp146) in the *M. leprae* thioredoxin reductase as the group exhibiting the p*K* value of 8.0 whose deprotonation abolishes activity. The pH dependence of V/K_{DTNB} observed for the MlTrxR−Trx catalyzed reduction of DTNB is similar to that for the maximum velocity, and the identification of the groups observed is the same as that discussed above.

Isotope Effect Studies. The reduction of quinones by flavoprotein reductases, including thioredoxin reductase, has been demonstrated not to involve reaction with the dithiols present on the two-electron-reduced flavoenzyme. Therefore, we did not expect, nor did we observe, any kinetically significant proton-transfer reactions using solvent kinetic isotope effect approaches. Large primary deuterium kinetic isotope effects were, however, observed on both V and V/K_{NADPH} in the reduction of naphthoquinone using either MlTrxR−Trx or MlTrxR (Table 2). The higher values of the V_{max} of NQ reduction compared to disulfide reduction (Table 1), and the absence of any solvent kinetic isotope effect, are consistent with the oxidation of the reduced enzyme by NQ, k_{ox}, being significantly faster than hydride transfer and enzyme reduction, k_{red}. This interpretation is supported by the near-equivalence of the steady-state rates of NQ reduction by MlTrxR−Trx and MlTrxR, and, more convincingly, by the close correspondence between the steady-state value of V_{max} for NQ reduction and the rate of enzyme reduction observed in pre-steady-state experiments (Table 3). It thus appears that the reductive half-reaction is rate-limiting in the reduction of NQ by either MlTrxR−Trx or MlTrxR.

The enzyme-catalyzed reduction of thioredoxin is a significantly slower overall reaction, with maximum steady-state rates of ca. 2 s^{-1}, compared to rates of 15 s^{-1} for quinone reduction (Table 1). The reduction of oxidized thioredoxin necessarily involves the redox-active disulfide of thioredoxin reductase with protonation of one or more of the thiolate moieties of the reduced Trx (Scheme 2). This disulfide exchange chemistry, occurring in the oxidative half-reaction, is slower than hydride transfer from NADPH to the flavin and subsequent electron rearrangement, based on the very modest magnitude of the primary kinetic isotope effects on the maximum velocity observed for this reaction (Table 2). This predicts that the proton-transfer steps occurring in the thioredoxin-reducing half-reaction will be slow relative to hydride transfer, and are expected to result in large solvent kinetic isotope effects. Our results support this hypothesis, and the ^{D2O}V values observed for the reduction of Trx by both MlTrxR−Trx and MlTrxR+Trx proteins are large (2.3−2.7, Table 2). To provide a basis for comparison, the solvent kinetic isotope effects on DTNB reduction were determined, using the fused MlTrxR−Trx. A similar value of the ^{D2O}V was observed for this reaction ($^{D2O}V_{DTNB}$ = 2.1), and, as expected, no $^{D2O}V/K_{DTNB}$ was observed (Figure 3) since the product of DTNB reduction, TNB^-, does not require protonation of the resonance-stabilized thiophenolate anion product. Analysis of the solvent isotopic composition dependence of the maximum velocity for DTNB reduction revealed a linear proton inventory, indicative of a single proton-transfer reaction occurring in the oxidative half-reaction. We propose that, by analogy to glutathione reductase (*37*), the proton transfer responsible for the observed ^{D2O}V occurs between the protonated aspartate general acid and thiolate anion of Trx. These data argue that protonation of the thiolate anion of Trx is a slow step in the oxidative half-reaction.

As expected for a pseudo-ping-pong kinetic mechanism, rate-limiting disulfide interchange chemistry would suggest that the reduction of the enzyme by NADPH would be fast, and that the primary deuterium kinetic isotope effect on this half-reaction would be attenuated. In fact, only modest primary deuterium kinetic isotope effects are observed using [4S-4-^{2}H]-NADPH as substrate (Table 2). Interestingly, the primary deuterium kinetic isotope effects on the maximum velocity, ^DV, exhibited by the reductase (MlTrxR) are slightly larger than the corresponding effects exhibited by the fused reductase−thioredoxin, MlTrxR−Trx (1.8 vs 1.1). This may reflect a subtle difference between the ratio of the two half-reaction rates catalyzed by the two enzymes.

Last, the primary deuterium kinetic isotope effects on V/K_{NADPH} are large and nearly equivalent to the corresponding isotope effects on V for NQ reduction, but are very small for the reduction of thioredoxin. Since it is likely that the intrinsic isotope effect on hydride transfer from NADPH to bound FAD is identical for MlTrxR−Trx and MlTrxR, and should be similarly unaffected by the nature of the reducible substrate (NQ or Trx), then this difference is curious. The magnitude of the observed $^DV/K_{NADPH}$ will depend on the intrinsic isotope effect (at least as large as 3.3−3.7) and the forward commitment factor for NADPH, defined here as the ratio of the rate of the hydride-transfer step to the rate of NADPH dissociation from the binary E−NADPH complex. In other flavoprotein disulfide reductases, the binary E−nucleotide complex is a single, structurally well-defined species. However, the unique and distinct three-dimensional structure of the thioredoxin reductase suggests that there may be multiple conformers of the E−NADPH complex, including those previously described as FO and FR conformers, distinguished by a large domain movement in the enzyme (11−15). Our data can most easily be accommodated by a model in which the presence of thioredoxin, either added to the reductase (MlTrxR+Trx) or covalently attached to the reductase (MlTrxR−Trx) influences the distribution of the enzyme in the two conformers, and by stabilizing the FR conformation, reduces the rate of NADPH dissociation. The net result of this change in conformer distribution is observed in the significantly smaller values of $^DV/K_{NADPH}$ exhibited during reaction with Trx compared to the same values observed during reaction with NQ. The more modest differences observed in the values of $^DV/K_{NADPH}$ observed for NQ reduction by MlTrxR or MlTrxR−Trx may similarly reflect smaller, but significant, differences in the conformer populations of the two enzymes.

Sodium Dithionite Titrations. The dithionite titration of the truncated form of TrxR from *M. leprae* is similar to the titration of *E. coli* TrxR, in that the flavin absorbance of MlTrxR is diminished gradually throughout. The titration required 2 equiv of dithionite per FAD, without formation of a unique spectral intermediate centered around 540 nm due to a thiolate−flavin charge-transfer complex (38−39) at the two-electron-reduced stage (*3*) as is observed in glutathione reductase and lipoamide dehydrogenase (*1*). This result shows that during the whole titration, reducing equivalents are distributed between the two redox centers, FAD and active site disulfide. This indicates only a small difference in the midpoint potentials between the FAD/$FADH_2$ couple and the disulfide/dithiol couple, as is the case for TrxR from *E. coli* (*25*−*27*). This small separation is also suggested in the titration of the fusion enzyme, MlTrxR−Trx.

AADP$^+$ Titrations. The mutant C138S of the *E. coli* TrxR is thought to be mostly in the FO conformation, since in a titration of this mutant with $AADP^+$ the FAD fluorescence is quenched only slightly. When the mutant is modified with phenylmercuric acetate, the steric hindrance of the phenylmercuric group attached to Cys135 forces the enzyme to adopt the FR conformation in which FAD is in close contact with the NADPH binding site. The FAD fluorescence is quenched significantly in a titration of the modified mutant with $AADP^+$ (*16*). In this study, only slight fluorescence quenching was observed in the $AADP^+$ titration of MlTrxR or MlTrxR−Trx. By analogy with *E. coli* TrxR, this suggests that both MlTrxR and MlTrxR−Trx favor a conformation which is similar to the FO conformation of the *E. coli* enzyme.

Rapid Reaction Studies. Wild-type TrxR from *E. coli* reacts with NADPH in three phases. The first phase, completed in the dead time of the instrument (∼3 ms), is the formation of an NADPH−FAD charge-transfer complex, which is observed as a slight drop of the flavin absorbance at 456 nm and appearance of a broad band centered at 570 nm. Flavin reduction begins in the next phase as evidenced by the absorbance decrease at 456 nm, accompanied by the appearance of another long-wavelength band centered at 690 nm due to formation of the $FADH_2$−$NADP^+$ charge-transfer

complex. The absorbance in the 456 nm region continues to decrease in the third phase which is thought to reflect further flavin reduction at a rate limited by the change between the FO and FR conformations. Thus, those enzyme molecules preexisting in the FR conformation, with the pyridinium and isoalloxazine rings juxtaposed, form the NADPH−flavin charge-transfer complex directly, followed by reduction (second phase); those molecules preexisting in the FO conformation must rotate prior to charge-transfer formation and reduction (third phase). C138S is reduced by NADPH in the same three phases, but the proportion of the reaction occurring in each phase is different from wild-type enzyme due to the fact that the FO conformation is favored in C138S while the FR conformation predominates in wild-type enzyme (*15*).

Data analysis for the reduction of MlTrxR by NADPH indicates that the reaction takes place in at least four phases (Figure 5). In the first phase, a long-wavelength band centered around 570 nm signals formation of the NADPH−FAD charge-transfer complex. Some flavin reduction occurs between 13 and 100 ms with the equilibrium level of the NADPH−FAD charge-transfer complex remaining virtually unchanged. Further reduction of the FAD takes place in at least three phases, leaving the enzyme slightly more than half-reduced. While the intermediates observed in the reduction of MlTrxR are the same as those seen with the *E. coli* enzyme, the reductive half-reactions in the two enzymes are quantitatively different (*15*). MlTrxR appears to be more highly regulated in the hydride transfer from NADPH to the FAD.

Conclusions. The pattern of reduction observed with MlTrxR−Trx and MlTrxR is very similar, indicating that the dithiol−disulfide interchange between TrxR and Trx is not detectable. We would suggest that with Trx tethered there is no urgency to reduce Trx until it is needed for other cellular processes. These (e.g., deoxyribonucleotide synthesis) would be slow in this organism having a low rate of cell division (*40*).

The present studies have provided a kinetic basis for the evaluation of potentially slow conformational changes which might distinguish the unique *M. leprae* fused thioredoxin reductase−thioredoxin from the well-studied and structurally characterized *E. coli* thioredoxin reductase. We have found that the kinetic properties of MlTrxR−Trx and MlTrxR are similar for the reduction of both Trx and NQ, but that DTNB reduction rates differ by more than 10-fold. The isotopic sensitivity of the two enzymes is qualitatively very similar, but the small differences noted may reflect a subtle change in the ratio of conformers. Finally, the pH dependence of the maximum velocity and V/K_{DTNB} are very different for the two enzymes, reflecting the very different reactivity of the reductase dithiols and the thioredoxin dithiols.

When the *E. coli* TrxR mutant C135S forms a stable cross-linked complex with the *E. coli* Trx mutant C32S, the enzyme is inactivated completely due to restriction of the enzyme in the FR conformation (Scheme 1) by the attached thioredoxin (*17*). As mentioned above, we hypothesized that the tethered Trx would impede rotation. In the case of the fusion enzyme MlTrxR−Trx, the peptide linker between the TrxR and Trx portions gives the enzyme some flexibility to permit the proposed conformational change making the fusion protein enzymatically active. However, the low activity of MlTrxR−Trx compared with *E. coli* TrxR suggests that the conformational change is not as free as it is in *E. coli* TrxR. Therefore, we expected to see higher activity and faster reduction by NADPH for the truncated enzyme that lacks the thioredoxin portion and the peptide linker. But the results of this study demonstrate a surprising similarity between MlTrxR−Trx and MlTrxR. We therefore conclude that the lower catalytic activity and the slow rate of reduction of MlTrxR−Trx by NADPH result primarily from intrinsic properties of the reductase and that the tethered Trx makes only a minor kinetic contribution.

ACKNOWLEDGMENT

We are grateful to Dr. Scott B. Mulrooney, University of Michigan, for reading the manuscript and for helpful suggestions, and to Ms. Donna M. Veine, VA Medical Center, Ann Arbor, for help with the manuscript.

REFERENCES

1. Williams, C. H., Jr. (1992) in *Chemistry and Biochemistry of Flavoenzymes* (Müller, F., Ed.) Vol. III, pp 121−211, CRC Press, Boca Raton.
2. Moore, E. C., Reichard, P., and Thelander, L. (1964) *J. Biol. Chem. 239*, 3445−3452.
3. Zanetti, G., and Williams, C. H., Jr. (1967) *J. Biol. Chem. 242*, 5232−5236.
4. Williams, C. H., Jr. (1995) *FASEB J. 9*, 1267−1276.
5. Thelander, L., and Reichard, P. (1979) *Annu. Rev. Biochem. 48*, 133−158.
6. Holmgren, A. (1985) *Annu. Rev. Biochem. 54*, 237−271.
7. Arscott, L. D., Gromer, S., Becker, K., Schirmer, R. H., and Williams, C. H., Jr. (1997) *Proc. Natl. Acad. Sci. U.S.A. 94*, 3621−3626.
8. Schulz, G. E., Schirmer, R. H., Sachsenheimer, W., and Pai, E. F. (1978) *Nature 27*, 120−124.
9. Arscott, L. D., Thorpe, C., and Williams, C. H., Jr. (1981) *Biochemistry 20*, 1513−1520.
10. Rietveld, P., Arscott, L. D., Perham, R. N., and Williams, C. H., Jr. (1994) *Biochemistry 33*, 13888−13895.
11. Kuriyan, J., Krishna, T. S. R., Wong, L., Guenther, B., Pahler, A., Williams, C. H., Jr., and Model, P. (1991) *Nature 352*, 172−174.
12. Waksman, G., Krishna, T. S. R., Williams, C. H., Jr., and Kuriyan, J. (1994) *J. Mol. Biol. 23*, 800−816.
13. Lennon, B. W., and Williams, C. H., Jr. (1995) *Biochemistry 34*, 3670−3677.
14. Lennon, B. W., and Williams, C. H., Jr. (1996) *Biochemistry 35*, 4704−4712.
15. Lennon, B. W., and Williams, C. H., Jr. (1997) *Biochemistry 36*, 9464−9477.
16. Mulrooney, S. B., and Williams, C. H., Jr. (1997) *Protein Sci. 6*, 2188−2195.
17. Wang, P.-F., Veine, D. M., Ahn, S.-H., and Williams, C. H., Jr. (1996) *Biochemistry 35*, 4812−4819.
18. Veine, D. M., Onishi, K., and Williams, C. H., Jr. (1997) *Protein Sci. 7*, 369−375.
19. Wieles, B., van Soolingen, D., Holmgren, A., Offringa, R., Ottenhoff, T., and Thole, J. (1995) *Mol. Microbiol. 16*, 921−929.
20. Wieles, B., van Noort, J., Drijfhout, J. W., Offringa, R., Holmgren, A., and Ottenhoff, T. H. M. (1995) *J. Biol. Chem. 270*, 25604−25606.
21. Holmgren, A. (1989) *J. Biol. Chem. 264*, 13963−13966.
22. Mitsui, A., Hirakawa, T., and Yodoi, J. (1992) *Biochem. Biophys. Res. Commun. 186* (3), 1220−1226.
23. Cleland, W. W. (1979) *Methods Enzymol. 63*, 103−138.
24. Stoll, V. S., and Blanchard, J. S. (1988) *Arch. Biochem. Biophys. 260*, 752−757.
25. Prongay, A. J., Engelke, D. R., and Williams, C. H., Jr. (1989) *J. Biol. Chem. 264*, 2656−2664.

26. Prongay, A. J., and Williams, C. H., Jr. (1992) *J. Biol. Chem. 267*, 25181−25188.
27. O'Donnell, M. E., and Williams, C. H., Jr. (1983) *J. Biol. Chem. 258*, 13795−13805.
28. Massey, V., Matthews, R. G., Foust, G. P., Howell, L. G., Williams, C. H., Jr., Zanetti, G., and Ronchi, S. (1970) in *Pyridine Nucleotide-Dependent Dehydrogenases* (Sund, H., Ed.) pp 393−409, Springer-Verlag, Berlin.
29. Williams, C. H., Jr., Prongay, A. J., Lennon, B. W., and Kuriyan, J. (1991) in *Flavins and Flavoproteins 1990* (Curti, B., Ronchi, S., and Zanetti, G., Eds.) pp 497−504, Walter de Gruyter, Berlin.
30. Tu, S.-C. (1981) *Arch. Biochem. Biophys. 208*, 487−494.
31. Cenas, N., Arscott, D., Williams, C. H., Jr., and Blanchard, J. S. (1994) *Biochemistry 33*, 2509−2515.
32. Marcinkeviciene, J., and Blanchard, J. S. (1995) *Biochemistry 34*, 6621−6627.
33. Marcinkeviciene, J., and Blanchard, J. S. (1997) *Arch. Biochem. Biophys. 340*, 168−176.
34. Mas, M. T., and Colman, R. F. (1984) *Biochemistry 23*, 1675−1681.
35. Mulrooney, S. B., and Williams, C. H., Jr. (1994) *Biochemistry 33*, 3148−3154.
36. Chivers, P. T., Prehoda, K. E., Volkman, B. F., Kim, B.-M., Markley, J. L., and Raines, R. T. (1997) *Biochemistry 36*, 14985−14991.
37. Wong, K. K., Vanoni, M. A., and Blanchard, J. S. (1988) *Biochemistry 27*, 7091−7096.
38. Matthews, R. G., and Williams, C. H., Jr. (1976) *J. Biol. Chem. 251*, 3956−3964.
39. Massey, V., and Ghisla, S. (1974) *Ann. N.Y. Acad. Sci. 227*, 446−465.
40. Shepard, C. C. (1971) *Bull. WHO 44*, 821−825.

BI980754E